computers

Article

A GIS-Based Fuzzy Model to Detect Critical Polluted Urban Areas in Presence of Heatwave Scenarios

Barbara Cardone [1], Ferdinando Di Martino [1,2,*] and Vittorio Miraglia [1]

[1] Department of Architecture, University of Naples Federico II, Via Toledo 402, 80134 Napoli, Italy; b.cardone@unina.it (B.C.); vittorio.miraglia@unina.it (V.M.)
[2] Center for Interdepartmental Research "Alberto Calza Bini", University of Naples Federico II, Via Toledo 402, 80134 Napoli, Italy
* Correspondence: fdimarti@unina.it; Tel.: +39-081-2538904

Abstract: This research presents a new method for detecting urban areas critical for the presence of air pollutants during periods of heatwaves. The proposed method uses a geospatial model based on the construction of Thiessen polygons and a fuzzy model based on assessing, starting from air quality control unit measurement data, how concentrations of air pollutants are distributed in the urban study area during periods of heatwaves and determine the most critical areas as hotspots. The proposed method represents an optimal trade-off between the accuracy of the detection of critical areas and the computational speed; the use of fuzzy techniques for assessing the intensity of concentrations of air pollutants allows evaluators to model the assessments of critical areas more naturally. The method is implemented in a GIS-based platform and has been tested in the city of Bologna, Italy. The resulting criticality maps of PM_{10}, NO_2, and $PM_{2.5}$ pollutants during a heatwave period that occurred from 10 to 14 July 2023 revealed highly critical hotspots with high pollutant concentrations in densely populated areas. This framework provides a portable and easily interpretable decision support tool which allows you to evaluate which urban areas are most affected by air pollution during heatwaves, potentially posing health risks to the exposed population.

Keywords: air pollutant; heatwave scenario; GIS; Thiessen polygons; APAS; fuzzy sets; fuzzy partitions

Citation: Cardone, B.; Di Martino, F.; Miraglia, V. A GIS-Based Fuzzy Model to Detect Critical Polluted Urban Areas in Presence of Heatwave Scenarios. *Computers* **2024**, *13*, 143. https://doi.org/10.3390/computers13060143

Academic Editors: Paolo Bellavista and Robertas Damaševičius

Received: 9 May 2024
Revised: 27 May 2024
Accepted: 3 June 2024
Published: 5 June 2024

1. Introduction

Urban air pollution is a leading cause of cardiorespiratory issues in citizens. Recent research estimates that the average air pollution in European cities has reduced life expectancy by about 2.2 years [1].

Recent studies aimed at evaluating which urban areas were most critical due to air pollution. In [2], a model was implemented on a GIS platform for the analysis of the types of urban patterns with lower ventilation potential that are, therefore, more critical in the presence of high concentrations of pollutants in the atmosphere. Urban patterns were detected considering an approach proposed in [3] for the determination of precinct ventilation zones based on three characteristics: urban form compactness, height of buildings, and patterns of streets. The model was tested for the cities of Antwerp in Belgium and Gdansk in Poland to detect which subzones were less ventilated and more exposed to polluting atmospheric agents.

A study of the most exposed urban patterns to air pollution based on land use classification is performed in [4]. Measures of ambient air quality parameters were obtained with portable digital air pollution detection devices, and spatial modeling methods were used to obtain maps of the distribution of each parameter in the metropolitan area of Kano, Nigeria. The results show that industrial and commercial areas are the most exposed to air pollution.

The existence of a close correlation between the growth of allergic respiratory diseases, such as rhinitis and bronchial asthma, air pollution, and the growth of average temperatures caused by global warming has been highlighted in [5].

An analysis of the impacts of global warming on health in urban settlements is carried out in [6]. The authors show that the main factors affecting citizens' respiratory problems are rising temperatures and air pollution.

It is very complex to try to determine a possible relationship between the presence of heatwaves and the increase in the concentration of air pollutants in cities due to the high number of variables to consider. For example, in the summer months in the presence of heatwaves, an increase in fire cases can generate an increase in the presence of harmful dust in the air; likewise, the excessive use of air conditioners in homes can lead to an increase in greenhouse gas emissions. Furthermore, during periods of intense heat, the increase in respiratory frequency in citizens, due to the body's adaptation to temperatures, can make people more exposed to air pollutants, creating serious health problems for individuals with previous respiratory problems.

This work aims to provide decision-makers and urban planners with a tool for evaluating urban areas in which the population is more exposed to health risks due to the presence of air pollutants during periods of heatwaves. These urban areas are identified as hotspots, where, in spatial analysis, a hotspot is an area of greater intensification of phenomena and exposure to risks. Recently, many studies focused on the detection of hotspots in urban analysis problems inherent to different problems in which the population is exposed to risks, such as soil pollution [7], earthquake disasters [8], crime analysis during pandemic periods [9], and traffic incident analysis [10].

To guarantee the portability of the proposed framework in different urban settlements, the model was built starting from generally available data, avoiding resorting to information on a more detailed scale, which is often not available from various sources.

For this purpose, the urban study area is initially divided into subzones made up of the census areas; as highlighted in [11], they are homogeneous zones in terms of urban characteristics and represent the atomic zones in which the census data on the resident population are acquired.

Furthermore, since the available data relating to the concentrations of pollutants in the area are generally acquired from fixed control units for monitoring the quality of the area managed by institutional environmental protection bodies, a process for estimating the spatial distribution of the concentration has been developed in the model of a pollutant by partitioning the study area into Thiessen polygons created using mass points made up of the positions of the monitoring units.

Various well-known spatial interpolation methods, as inverse distance weighting, nearest neighbor, kriging and land use regression models [12], can be executed to assess the spatial distribution of pollutants. Reviews of these methods applied for urban air pollution monitoring are given in [13,14]. However, spatial interpolation methods are unsuitable if the monitoring units positioned in the urban study area are fixed, as the number of measurement points input to the interpolation process is small. In fact, many municipal public bodies are not equipped with mobile monitoring units, such as, for example, drone-based air quality systems, which allow for the periodic measurement of pollutant concentrations in different points of a city, and the pollutant measures are registered only from fixed monitoring units.

In [15], an air quality prediction model to study the distribution of air pollution parameters measured by wireless fixed monitoring units is proposed. Thiessen polygons are constructed based on the location of the monitoring units by assigning to each point included in a Thiessen polygon the values measured by the corresponding monitoring units. The authors tested this model in Shanghai, China, producing thematic maps of the distribution of an air quality index. A similar model is applied in [16] to assess the distribution of the $PM_{2.3}$ air pollutant in the city of Delhi, India.

Recently, many deep learning forecasting methods based on long short-term memory (LSTM) networks are applied to forecast air pollutant concentrations and their spatial distribution [17–20]. These models have the advantage of learning long-term dependencies on air pollution data. The results show increases in accuracy compared to two traditional approaches. However, these models are computationally expensive, and metaheuristic methods are often used to find the best hyperparameters for LSTM [21].

A problem of using these approaches for predicting the trend of pollutants in urban areas of study during periods of heatwaves is the determination of the training set, since, due to recent climate changes, the historical data of the concentrations of air pollutants in urban settlements during periods of intense heatwaves are only recent.

We propose a GIS-based fuzzy model to analyze the spatial distribution of air pollutants in urban areas during heatwaves. In our model, we consider an atomic subzone of the area of study given by the intersection between a census zone and a Thiessen polygon. This atomic subzone, called the Air Pollution Atomic Subzone (APAS), will be attributed estimates of the concentrations of pollutants determined, starting from the values measured by the corresponding monitoring station during a heatwave period, and an estimate of the resident population, determined by considering the population data in the census zone in which the APAS is included.

Estimates of pollutant concentrations are made by assigning a fuzzy linguistic label to the pollutant concentration. The use of fuzzification processes of air pollution measurements has the advantage of facilitating the use of the expert's approximate reasoning in the monitoring and evaluation of air quality in urban settlements. Fuzzifications of air pollutant data are used in a fuzzy inference model in [22] to assess the air quality in the urban area around Mexico City, Mexico, and in a fuzzy time series predictive model proposed in [23] to assess the air quality distribution in the city of Klang in Malaysia.

In the proposed method, the fuzzification of the air pollutant measures is accomplished through the creation by the decision-maker of a fuzzy partition of the measurement domain of the pollutant concentration in three fuzzy sets, termed, respectively, *Low*, *Medium*, and *High*, built using triangular fuzzy numbers. The APASs will be classified into three classes corresponding to the labels of the three fuzzy sets.

This approach of the fuzzification of the value of the concentration of the pollutant facilitates, on the one hand, the analysis of the decision-maker because it makes the interpretation of the distribution of the pollutant along the study area more effective and closer to their way of reasoning, and on the another, it simplifies the use of the framework, natively allowing the decision-maker to construct the fuzzy partitions using triangular fuzzy sets.

After dissolving adjacent APASs belonging to the same class, classified as hotspots for the analyzed air pollution, the dissolved subzones are classified as *High*. A criticality map of the hotspots is created by the decision-maker based on the population at risk residing in the hotspot.

By analyzing the criticality maps of each air pollutant, the decision-maker can evaluate which subzones of the urban study area must be given priority attention to safeguard the population that resides there.

The main strengths of the proposed framework are as follows:

- It provides the decision-maker with decision support for evaluating the most critical urban areas due to air pollution in periods of heatwaves and the resident population whose health is most at risk;
- It guarantees the portability of the model to different urban settlements requiring only census and monitoring data from monitoring stations provided by the relevant bodies;
- It has a high usability determined by the use of a fuzzification approach of the pollutant concentration values, which allows the decision-maker to make an interpretation of the distribution of the pollutant concentration closer to their way of reasoning.

In the following section, a detailed description of the proposed framework is provided, and the case study used for testing is presented. The results of the experimental tests are presented and discussed in Section 3, followed by a concluding discussion in Section 4.

2. Materials and Methods

The aim of the proposed GIS-based framework is to detect urban hotspots based on the high concentration of air pollutants during periods of heatwaves and to create a criticality map in which the critical hotspots are highlighted, i.e., the hotspots in which residents live in numbers exceeding a critical threshold. The user of the framework is a decision-maker who intends to evaluate in which urban areas in a specific heatwave period high values of air pollutants were detected, enough to put the health of residents at risk.

The method is schematized in Figure 1, where the variable corresponding to the concentration of an air pollution is labeled as a parameter. The method is composed of three phases.

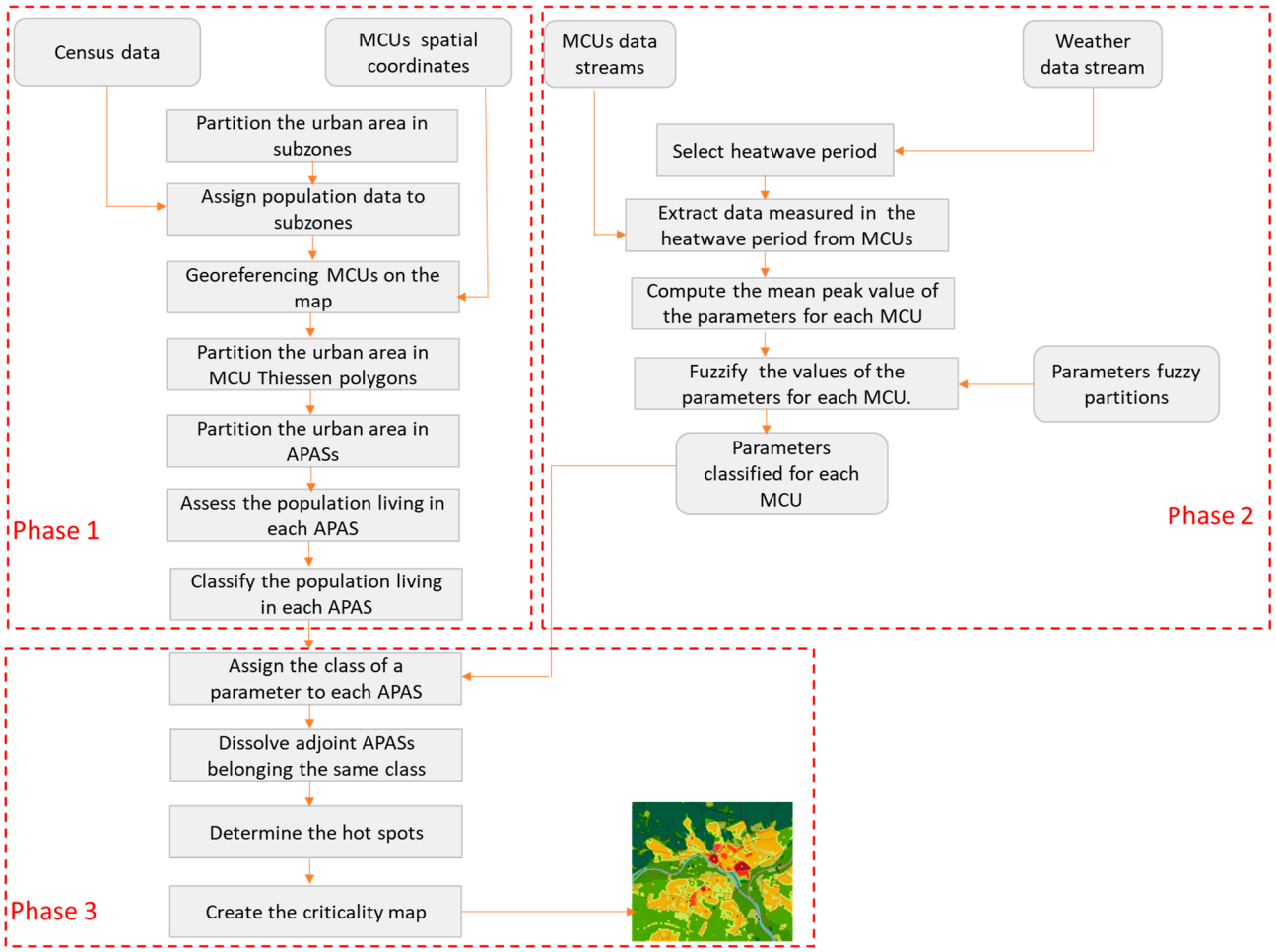

Figure 1. Flow diagram of the proposed method.

Below the phases of the process are described.

Phase 1—Partitioning the area of study in Air Pollution Atomic Subzones

Initially, the urban area of study is divided into subzones, corresponding to the population census areas. The reason for this partitioning is that a census area represents a homogeneous area in terms of urban and morphological characteristics and represents the surface unit for collecting census data [24,25].

The air quality measurement data are recorded by monitoring stations located along the study area, called Monitor Control Units (MCUs); they are georeferenced as points on

the map. The search for the heatwave period is carried out by analyzing the data acquired from weather stations located in or near the study area.

Then, the area of study is partitioned into Thiessen polygons, where the i*th* Thiessen polygon is given by the surface within which the closest MCU is the i*th* MCU. The spatial intersection of a Thiessen polygon with a subzone forms an atomic homogeneous area in terms of population data and air pollutant measures, called Air Pollution Atomic Subzones (APASs).

Based on the type of analysis they intend to carry out, the decision-maker chooses a population to consider in the analysis which is at risk (for example, all residents, or elderly people over 74, who may be more exposed to risks to their health).

To assess the population living in an APAS, it is supposed that the population is equally distributed in the corresponding subzone; in this way, the population resident in the APAS is approximated as a whole value equal to the product of the population of the subzone by the ratio between the area of the APAS and that of the subzone.

Finally, the population density of each APAS is classified. Based on the variation in and spatial distribution of residents, the decision-maker can categorize the population density as *Low*, *Medium*, and *High*.

Phase 2—Fuzzification of measurement values of air pollutant parameters for each MCU during a heatwave period

From the MCU data streams, the values of the parameters associated with the presence of pollutants are extracted and measured during the heatwave period. Then, the mean peak value of each parameter is calculated.

Formally, let $\{d_1, \ldots, d_n\}$ be the days of heatwave detected and let $\{m_i^j(t_{1_{d_h}}), \ldots, m_{ih}^j(t_{N_{d_h}})\}$ be the set of N measures of the i*th* parameters performed from the j*th* MCU in the day d_h, where h = 1, …, *n*. With $p_i^j\left(d_h\right)$ is denoted the max value of these N measures, i.e., the peak value measured for the i*th* parameter in the day d_h. The mean peak value of the i*th* parameter obtained in the period from the j*th* MCU is given by the following:

$$v_i^j = \frac{1}{n}\sum_{k=1}^{n} p_i^j(d_h) \tag{1}$$

This value is fuzzified by creating a fuzzy partition of the numerical domain of the i*th* parameter. The fuzzy partition on the domain of a parameter is built considering three fuzzy sets, labeled *Low*, *Medium*, and *High*, given, respectively, by an R-function, a triangular, and L-function fuzzy numbers given by the following membership functions:

$$\mu_{Low}(x) = \begin{cases} 1 & x < a_L \\ \frac{(b_L - x)}{b_L - a_L} & a_L \le x \le b_L \\ 0 & x > b_L \end{cases} \tag{2}$$

$$\mu_{Medium}(x) = \begin{cases} 1 & x < a_M \\ \frac{(x - a_M)}{b_M - a_M} & a_M \le x \le b_M \\ \frac{(c_M - x)}{c_M - b_M} & b_M \le x \le c_M \\ 0 & x > c_M \end{cases} \tag{3}$$

$$\mu_{High}(x) = \begin{cases} 0 & x < a_H \\ \frac{(x - a_H)}{b_H - a_H} & a_H \le x \le b_H \\ 1 & x > b_H \end{cases} \tag{4}$$

The numbers $a_L, b_L, a_M, b_M, c_M, a_H, b_H$ of the three fuzzy sets are fixed by the decision-maker for each primary pollutant by considering the recommended maximum values in the last World Health Organization (WHO) air quality guidelines (AQGs) published in the

year 2021 [26], which are the levels recommended to reduce risks to people's health. They are shown in Table 1.

Table 1. Recommended maximum values of the primary pollutants in the WHO AQGs ($\mu g/m^3$).

Pollutant	Averaging Period	AQG Level
$PM_{2.5}$	1 day	15 [1]
	Calendar year	5
PM_{10}	1 day	45 [1]
	Calendar year	15
O_3	Maximum daily 8 h mean	100 [1]
	Peak season	60
NO_2	1 h	200
	1 day	25 [1]
	Calendar year	10
SO_2	10 min	500
	1 day	40 [1]
CO	1 h	30
	Maximum daily 8 h mean	10
	1 day	4 [1]

[1] 99th percentile (3–4 exceedance days per year).

The numbers of the three fuzzy sets are linked to the Ruspini constraint [27] for the fuzzy partition, which imposes that for each x, the sum of the membership degrees to the three fuzzy sets $\mu_{Low}(x) + \mu_{Medium}(x) + \mu_{High}(x)$ is equal to 1, and that at least a membership degree is not equal to zero. The mean pick value of a parameter is fuzzified, assigning to it the label of the fuzzy set to which it belongs with the highest membership degree.

As an example, Figure 2 shows a Ruspini fuzzy partition of the parameter CO, in which the following are set: $a_L = 1, b_L = 2.5, a_M = 1, b_M = 2.5, c_M = 4, a_H = 2.5, b_H = 4$.

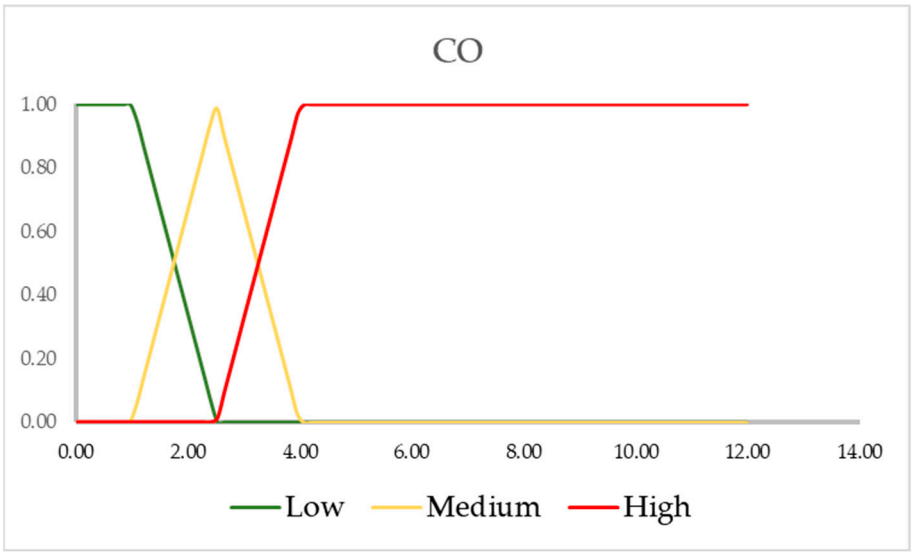

Figure 2. Example of fuzzy partition for the parameter CO.

Let the value $v^j_{CO} = 3.65\ \mu g/m^3$ be the mean peak value of CO obtained from the *jth* MCU. We obtain the following: $\mu_{Low}\left(v^j_{CO}\right) = 0.00$, $\mu_{Medium}\left(v^j_{CO}\right) = 0.23, \mu_{High}\left(v^j_{CO}\right) = 0.77$. Since the highest membership degree value is 0.77, this mean peak value is fuzzified, and the parameter measured by the MCU is classified as *High*.

Phase 3—Parameter hotspot detection and creation of the criticality map

In this phase, the decision-maker analyzes the distribution of a parameter in the study area and the detected hotspots. Each APAS is classified as *Low*, *Medium*, and *High*, both based on the resident population and the concentration of the air pollutant analyzed.

The APAS is assigned the concentration class of the parameter assigned to the corresponding MCU.

Then, adjoint APASs belonging to the same population class and the same parameter class are dissolved to form polygons; the polygons classified with the *High* parameter concentration are labeled as hotspots, that is, areas where during the heatwave period, the concentrations of the air pollutant analyzed are worrying for the health of residents.

To determine the most critical hotspots, the decision-maker categorizes them into different criticality levels based on the population density in each hotspot. The higher the criticality level, the higher the population density and the greater the need for attention and priority for intervention. Subsequently, a final criticality thematic map is created, classifying the APASs in the hotspot regions according to their criticality level. This classification considers the four criticality levels outlined in Table 2.

Table 2. Classification of the criticality level.

Criticality Level	Description
Low	Not hotspot zones
Medium	Hotspots in which the population density is Low
High	Hotspots in which the population density is Medium
Very High	Hotspots in which the population density is High

The zones not labeled as hotspots will be classified with criticality level Low. In these areas, there is no particular risk to the health of the inhabitants due to the concentration of the pollutant, regardless of the population density. The hotspots will be classified as *Medium* if the mean population density is *Low*, *High* if the mean population density in it is *Medium*, and *Very High* if it is *High*.

Algorithm 1 schematizes phase 1 in pseudocode, in which the area of study is partitioned in APASs.

Algorithm 1 APASs spatial data creation.

Input: Area of study
Census zone of the area of study
Population census data
Localization of the MCUs

Output: Spatial dataset containing the APASs

1. Partition the urban area of study in subzones given by the census zones
2. **For** each subzone s
3. Assign to z the corresponding population census data
4. **Next** subzone
5. Partition the area of study in Thiessen polygons starting from the localizations of the MCUs
6. Intersect the subzones with the Thiessen polygons to obtain the APASs
7. **For** each APAS *ap*
8. Assess the population living in *ap*
9. Calculate the population density living in *ap*
10. Classify the population density living in *ap*
11. **Next** APAS
12. **Return** the spatial dataset containing the APASs

Below, phase 2 is schematized in pseudocode, corresponding to the preprocessing activity needed to create the dataset containing the classification of the parameters for each MCU (Algorithm 2).

Algorithm 2 MCU parameters classification in a heatwave period.

Input: Wheater data stream for the area of study
MCUs data stream
Fuzzy partitions of the parameters

Output: MCUs dataset with the classification of the parameters

1. Set the heatwave period
2. **For** j = 1 to number of MCUs
3. **For** i = 1 to number of parameters
4. Compute the mean peak value of the i*th* parameter for the j*th* MCU v_i^j by (1)
5. Fuzzify v_i^j based on the fuzzy partition of the i*th* parameter
6. Classify the i*th* parameter for the j*th* MCU
7. **Next** i
8. **Next** j
9. **Return** the MCUs dataset with the classification of each parameter

Algorithm 3 schematizes in pseudocode phase 3, in which, for assigned parameter p, the hotspots are determined and the criticality map is created. Algorithm 3 is executed every time the decision-maker intends to detect hotspots and create a criticality map for an air pollutant.

Algorithm 3 Parameter criticality map creation.

Input: Parameter p
Spatial dataset containing the APASs
MCUs dataset with the classification of the parameters

Output: Criticality map

1. Extract the class assigned to the parameter p for each MCU
2. **For** each APAS ap
3. Assign to ap the class to which belongs the parameter p, set for the corresponding MCU
4. **Next**
5. Dissolve adjoint APASs belonging to the same class
6. **For** each dissolved APAS *apd*
7. **If** ad is classified as High
8. Annotate *apd* as a hotspot
9. Compute the population living in the hotspot *apd*
10. **End if**
11. **Next** ad
12. Create the criticality map based on the density of residents living in the hotspots
13. **Return** the criticality map

The Case Study

The case study focuses on the city of Bologna, Italy. As shown in Figure 3, Bologna is divided into six districts: Borgo Panigale–Reno, Navile, Porto–Zaragoza, San Donato–San Vitale, Santo Stefano, and Savena.

There are three Monitor Control Units; they take the same name as the address where they are located: one is located in Via Chiarini in the district of Borgo Panigale–Reno, one is located in Porta San Felice in the district of Porto–Zaragoza, and one is located at the Margherita Gardens in the district of Santo Stefano.

In Table 3, all the pollution parameters measured for each MCU are grouped.

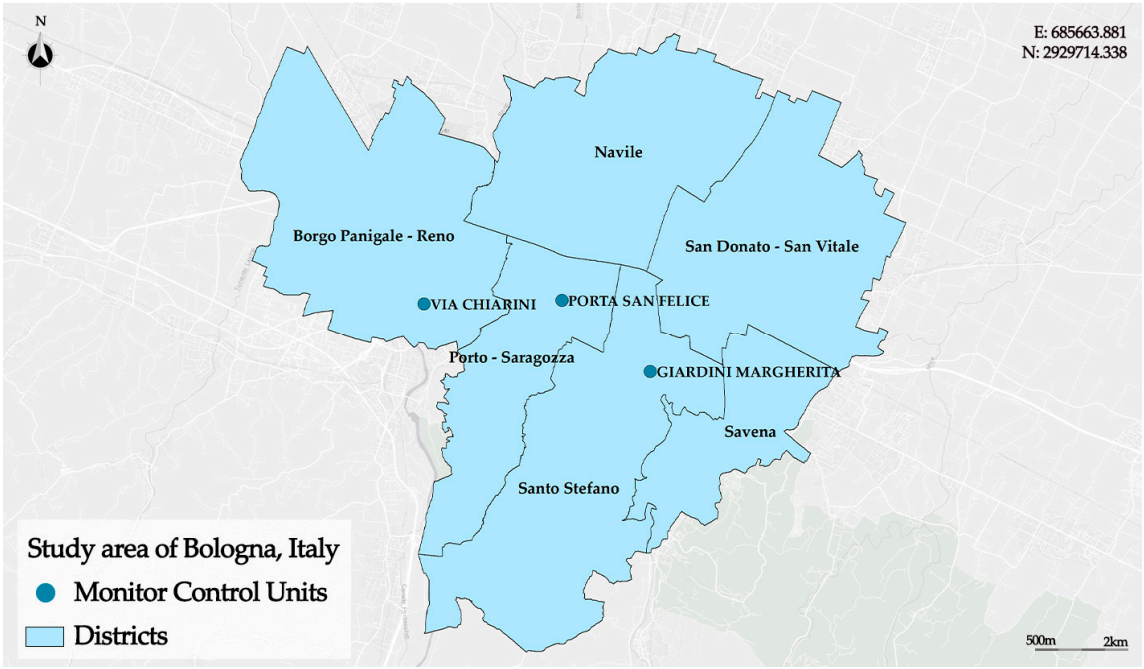

Figure 3. Framing of the study area and location of the three Monitor Control Units in Bologna, Italy.

Table 3. All of the pollutant parameters categorized for each MCU.

MCU	Parameter	Measurement Unit
Giardini Margherita	NO_2	$\mu g/m^3$
	O_3	$\mu g/m^3$
	$PM_{2.5}$	$\mu g/m^3$
	PM_{10}	$\mu g/m^3$
Porta San Felice	C6H6	$\mu g/m^3$
	CO	$\mu g/m^3$
	NO	$\mu g/m^3$
	NO_2	$\mu g/m^3$
	NOX	$\mu g/m^3$
	$PM_{2.5}$	$\mu g/m^3$
	PM_{10}	$\mu g/m^3$
Via Chiarini	NO_2	$\mu g/m^3$
	O_3	$\mu g/m^3$
	PM_{10}	$\mu g/m^3$

3. Results

The tests were carried out taking into account the period from 10 to 14 July 2023, in which a heatwave was detected, by checking the measured meteorological data.

The framework was implemented in the GIS platform ESRI ArcGIS Pro; the code was generated in the Python environment using the Spyder IDE for Python and the ESRI Python library. The air quality monitoring data were extracted from the repository of the Arpae—Regional Agency for Prevention, Environment and Energy of Emilia-Romagna (Italy), accessible on the website: https://dati.arpae.it/dataset/qualita-dell-aria-rete-di-monitoraggio, accessed on 1 May 2024.

The framework was tested to obtain the criticality maps of the parameters $PM_{2.5}$, PM_{10}, and NO_2. PM_{10} and NO_2 are measured by all three MCUs, while $PM_{2.5}$ is recorded only by the two control units Giardini Margherita and Porta San Felice.

The graphs in Figures 4 and 5 show, respectively, the daily trends of the $PM_{2.5}$, PM_{10}, and NO_2 parameters measured in the month of July 2023 from the MCUs Giar-

dini Margherita and Porta San Felice. Figure 6 shows the trend of PM_{10} and NO_2 measured in the month of July 2023 from the MCUs Via Chiarini. The period in which the heatwave was detected is highlighted in red.

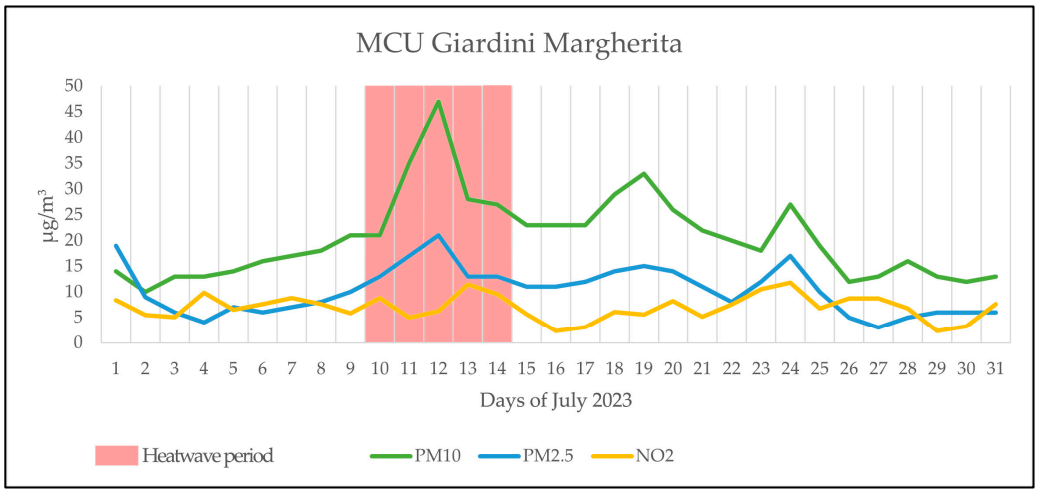

Figure 4. Giardini Margherita MCU—daily trends of $PM_{2.5}$, PM_{10}, and NO_2.

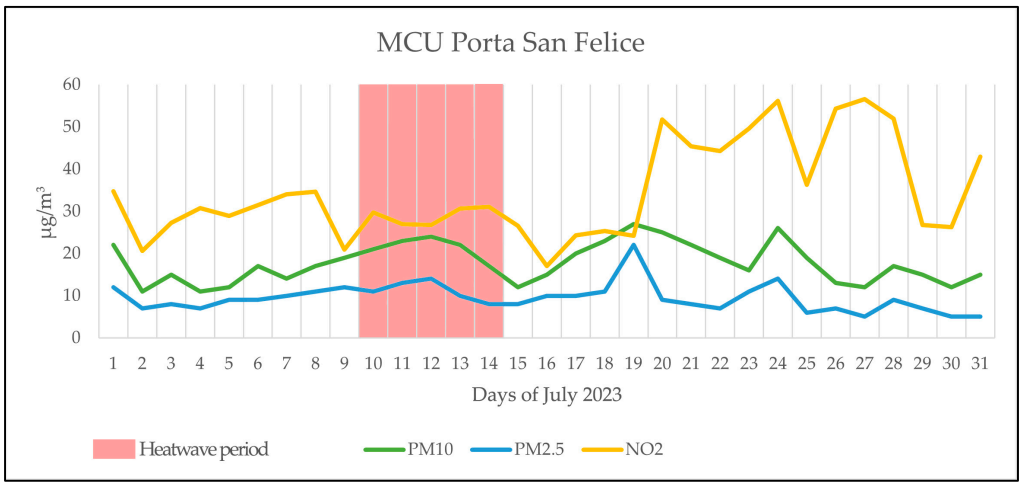

Figure 5. Porta San Felice MCU—daily trends of $PM_{2.5}$, PM_{10}, and NO_2.

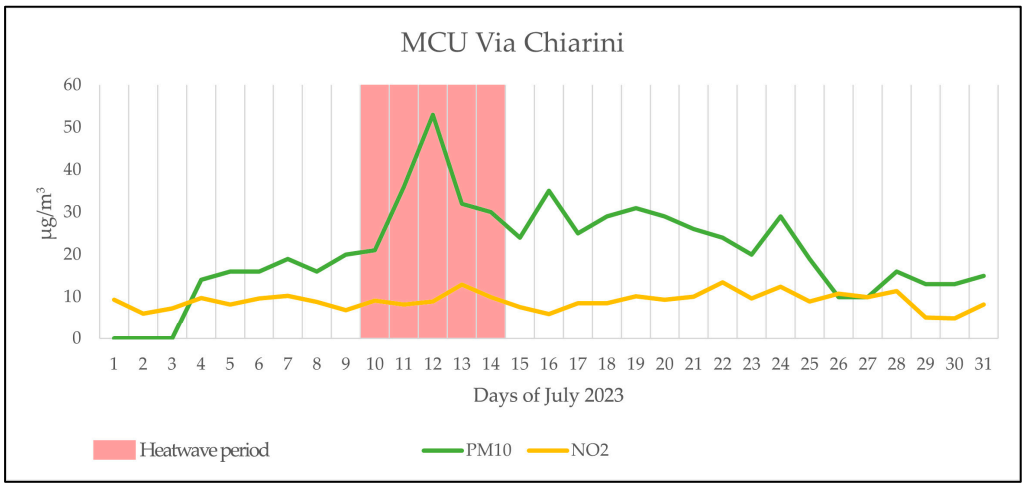

Figure 6. Via Chiarini MCU—daily trends of PM_{10} and NO_2.

During the heatwave period, the daily values of PM_{10} measured in the MCUs Giardini Margherita and Via Chiarini show peaks; on the contrary, these peaks are not present in the trends of the parameters measured by the MCU Porta San Felice. $PM_{2.5}$ also shows a peak in the trend of measurements made by the MCU Giardini Margherita, but it is less evident than the peak of PM_{10}. On the contrary, in the trend of the values measured by all three MCUs in the heatwave period, NO_2 does not show any significant variation. Furthermore, the daily NO_2 values measured by the MCU Porta San Felice are much higher than those measured by the other two MCUs.

Table 4 highlights the peak values above the WHO AQG thresholds recorded in the period by the MCUs. The alarm values are highlighted in bold.

Table 4. Maximum values recorded above the alarm thresholds in the heatwave period.

Parameter	WHO AQGs.	MCU	Maximum Value
PM_{10}	45.00	Via Chiarini	**53.00**
		Giardini Margherita	**47.00**
NO_2	25.00	Porta San Felice	**52.00**
$PM_{2.5}$	15.00	Giardini Margherita	**21.00**

To obtain the criticality maps of PM_{10} and NO_2, Thiessen polygons determined concerning three points made up of three MCUs are generated. Instead, to obtain the criticality maps of $PM_{2.5}$, it was necessary to regenerate Thiessen polygons, considering only two points corresponding to the two MCUs of Giardini Margherita and Porta San Felice. The APASs are obtained in the two cases as spatial intersections of the census zones with the Thiessen polygons. The map in Figure 7a shows the APASs built to obtain the criticality maps of PM_{10} and NO_2, while the map in Figure 7b shows the APASs built to obtain the criticality map of $PM_{2.5}$.

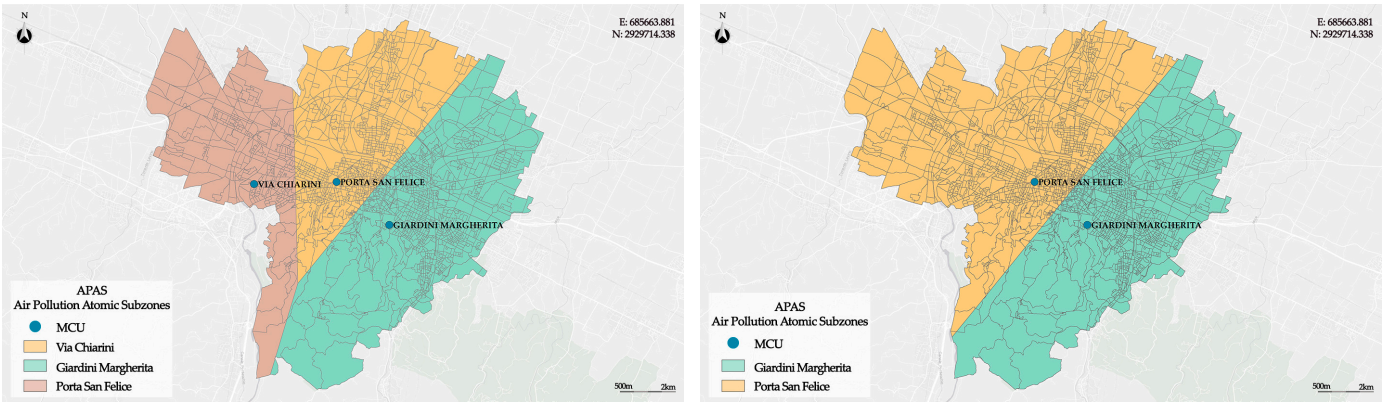

Figure 7. (**a**) APASs generated to evaluate the spatial distribution of PM_{10} and NO_2; (**b**) APASs generated to evaluate the spatial distribution of $PM_{2.5}$.

To classify the density of residents living in the APAS, a fuzzy partition was created consisting of three fuzzy sets, labeled *Low*, *Medium*, and *High*. This classification considers a range from the minimum to the maximum population density values in the census areas. The minimum value is 0, representing census areas without inhabitants, and the maximum value is 49,254 inhabitants per square kilometer.

The population density in an APAS is categorized as *Low*, *Medium*, or *High* based on the fuzzy set with the highest membership degree. The population density fuzzy partition is illustrated in Figure 8.

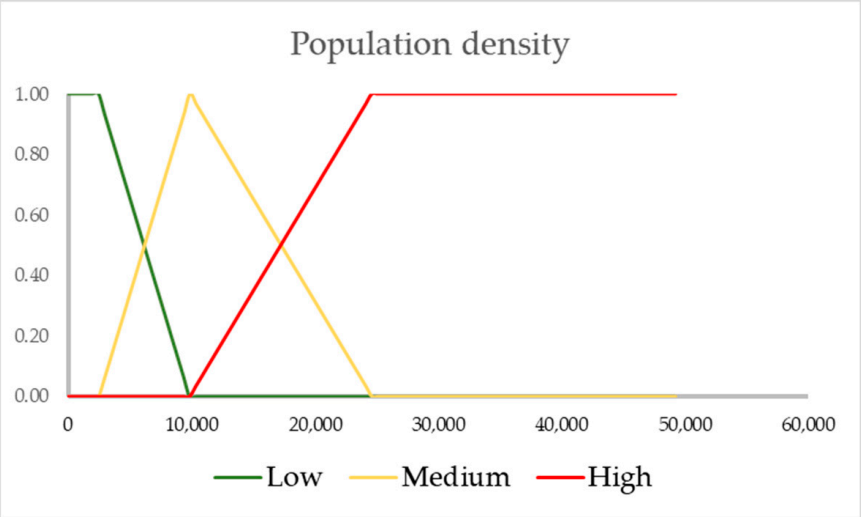

Figure 8. Fuzzy partition of the population density.

Figure 9a,b show the spatial distributions of the population density for the APASs generated to analyze, respectively, PM_{10} and NO_2 (Figure 9a) and $PM_{2.5}$ (Figure 9b).

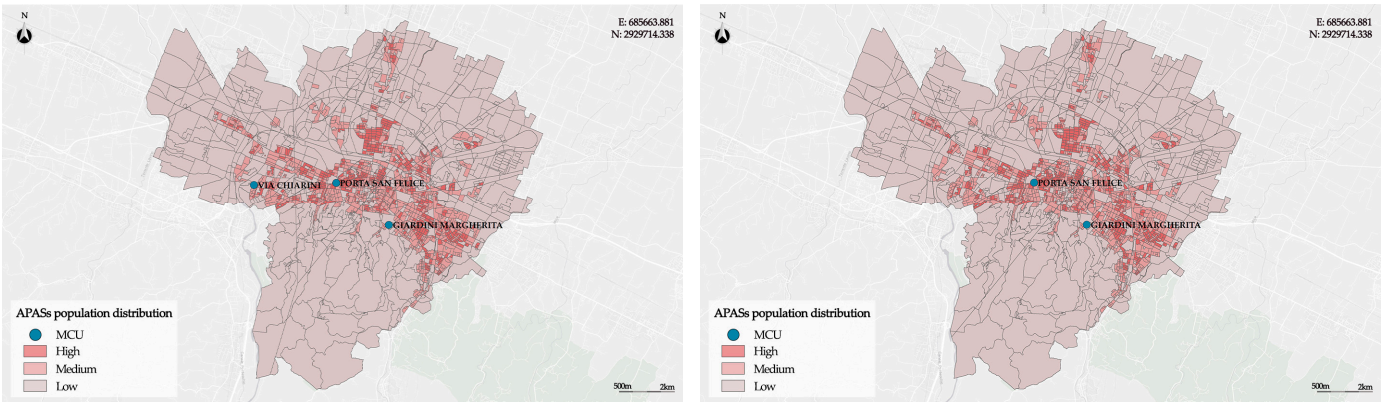

(**a**) (**b**)

Figure 9. (**a**) Population density of the APASs generated to evaluate the spatial distribution of PM_{10} and NO_2; (**b**) population density of the APASs generated to evaluate the spatial distribution of $PM_{2.5}$.

The two population density maps are similar. They show a greater presence of APASs with *High* population density in the central area of the city, while in all APASs located in the southern area of the city, the population density is *Low*.

For each MCU, the average values of the parameters are calculated in the heatwave period recorded in the city of Bologna. Then, these values are classified, and the processes needed to determine the criticality maps of each parameter are executed. They are described for each parameter in the following subparagraphs.

3.1. PM_{10} Criticality Map Creation

The fuzzification process is started by building a fuzzy partition into three fuzzy sets of PM_{10}, where the fuzzy sets are given, respectively, by an R-function, a triangular, and an L-function fuzzy number. It was created with the help of a domain expert, taking into consideration the recommended maximum values indicated in the WHO AQGs.

Figure 10 shows the fuzzy partition of PM_{10}.

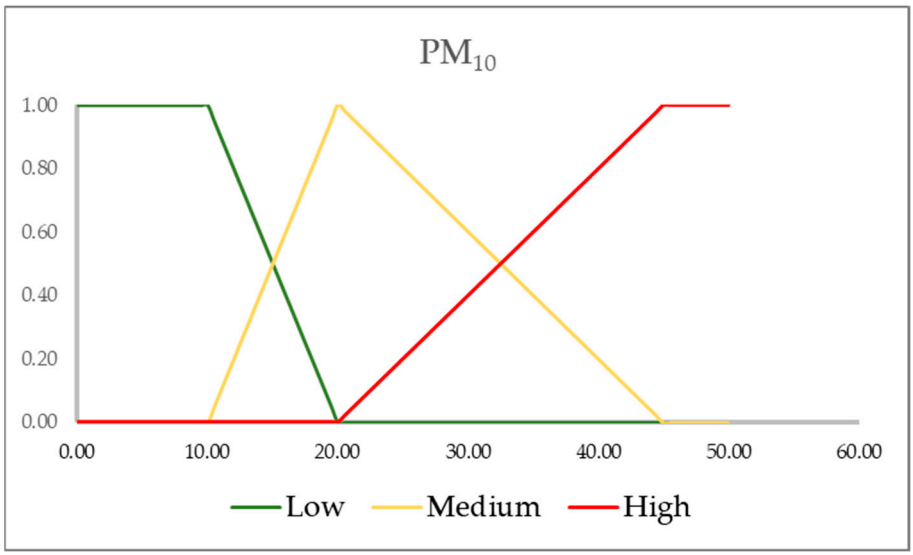

Figure 10. Fuzzy partition of PM_{10}.

After the fuzzification process, each of the three MCUs is classified with the label of the fuzzy set to which it belongs with the highest membership degree. Then, the APASs are classified by the class assigned to the correspondent MCU.

After dissolving bordering APASs belonging to the same PM_{10} concentration class, the zones classified with a PM_{10} concentration of High are detected as hotspots.

Finally, the PM_{10} criticality map is created considering the criticality levels described in Table 2. Figure 11 shows the criticality map of PM_{10}.

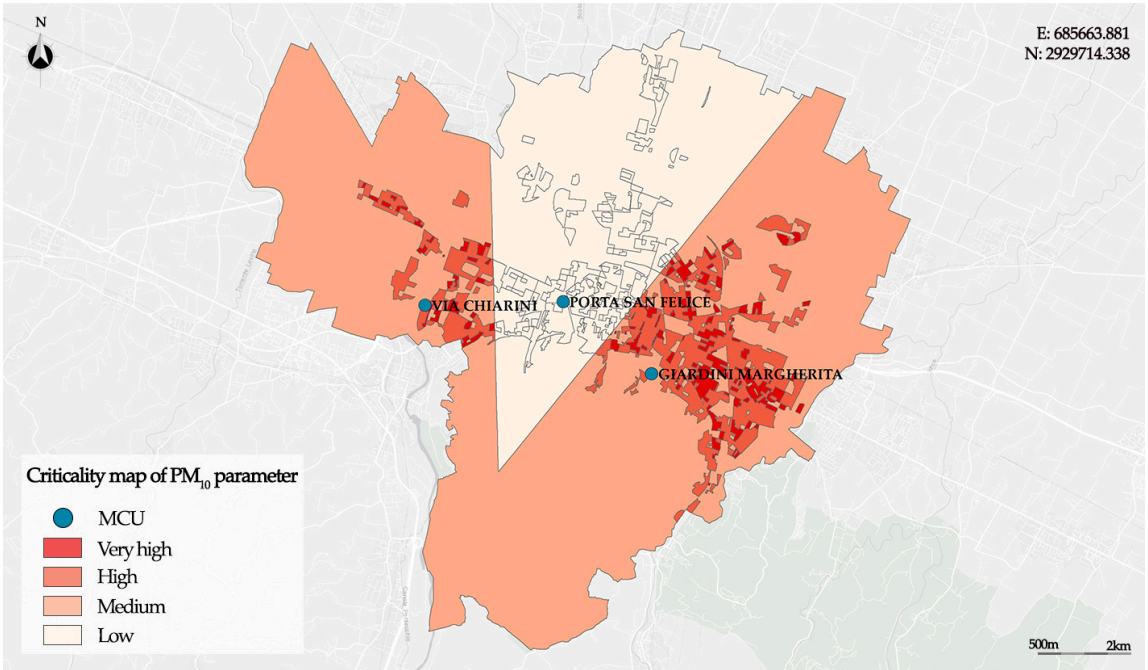

Figure 11. Criticality map of PM_{10}.

Only the areas included in the Thiessen polygon associated with the Porta San Felice MCU are not hotspots and are classified as having a *Low* criticality level. The areas to the south of the city, where the population density is *Low*, are classified as having a *Medium* criticality level, as in these areas the concentration of PM_{10} is *High*. The other areas, located mainly in the central area of the city, are hotspots classified as having a *High* criticality

level, where the population density is *Medium*, and as having a *Very High* level, where the population density is *High*. These represent the most critical areas in which interventions to protect the population are a priority.

3.2. NO_2 Criticality Map Creation

The NO_2 parameter is also measured by all three MCUs. The corresponding fuzzy partition is given by the three fuzzy sets *Low*, *Medium*, and *High* shown in Figure 12, considering the maximum values indicated in the WHO AQGs.

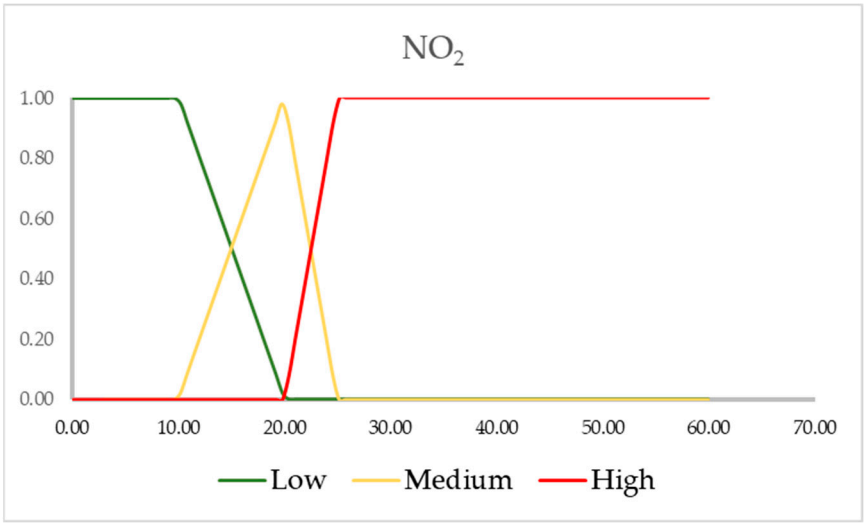

Figure 12. Fuzzy partition of NO_2.

Executing the process described previously, the zones classified with the NO_2 concentration *High* are detected as hotspots.

Finally, the NO_2 criticality map is processed based on the criticality levels described in Table 2. Figure 13 shows this criticality map.

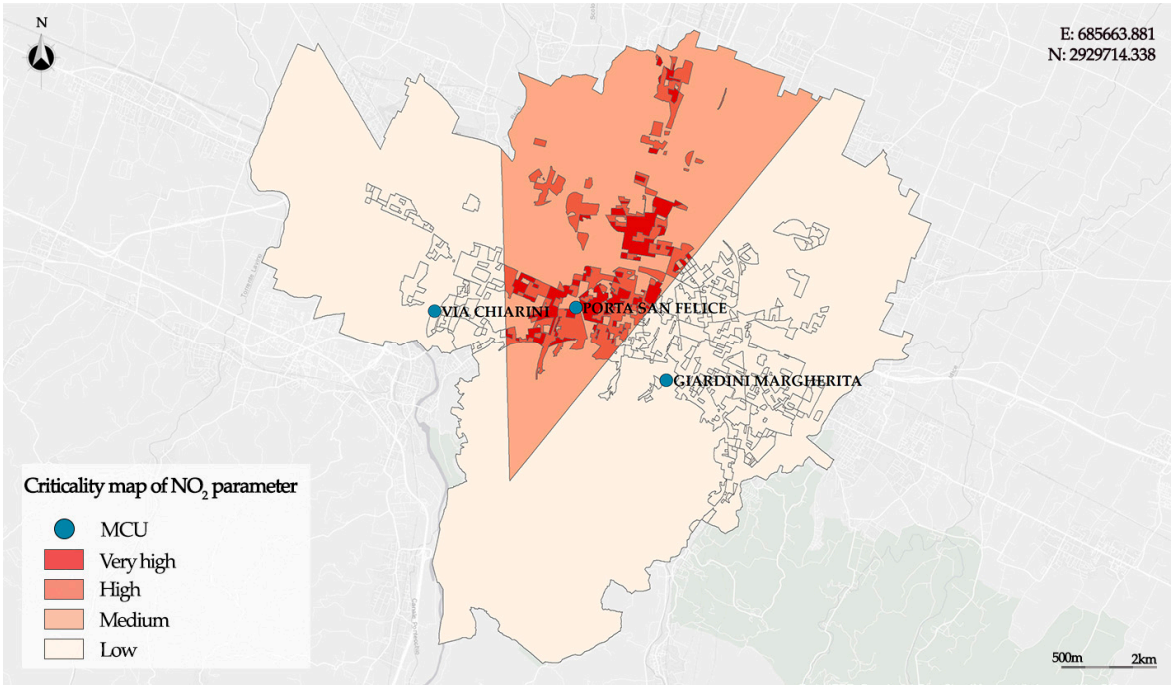

Figure 13. Criticality map of NO_2.

The spatial distribution of the criticality level appears to be the opposite of that of PM_{10}. The areas included in the Thiessen polygons associated with the MCUs Via Chiarini and Giardini Margherita are not hotspots and are classified with the *Low* criticality level. On the contrary, the areas included in the Thiessen polygon associated with the MCU Porta San Felice are hotspots, mainly classified with criticality level *Medium*. Some of these areas, located mainly in the central area of the city, are classified with criticality level *High* or *Very High*, as the population density in them is *Medium* or *High*.

This spatial distribution of the criticality map of NO_2, inverse to that of PM_{10}, is probably due to the presence of anthropic elements, such as, for example, excessively used air conditioners, which causes the intensification of the NO_2 concentration in heatwave periods.

3.3. $PM_{2.5}$ Criticality Map Creation

The $PM_{2.5}$ pollutant is measured only by the two MCUs Porta San Felice and Giardini Margherita. The fuzzy partition of the parameter is given by the three fuzzy sets *Low*, *Medium*, and *High*, shown in Figure 14, considering the maximum values indicated in the WHO AQGs.

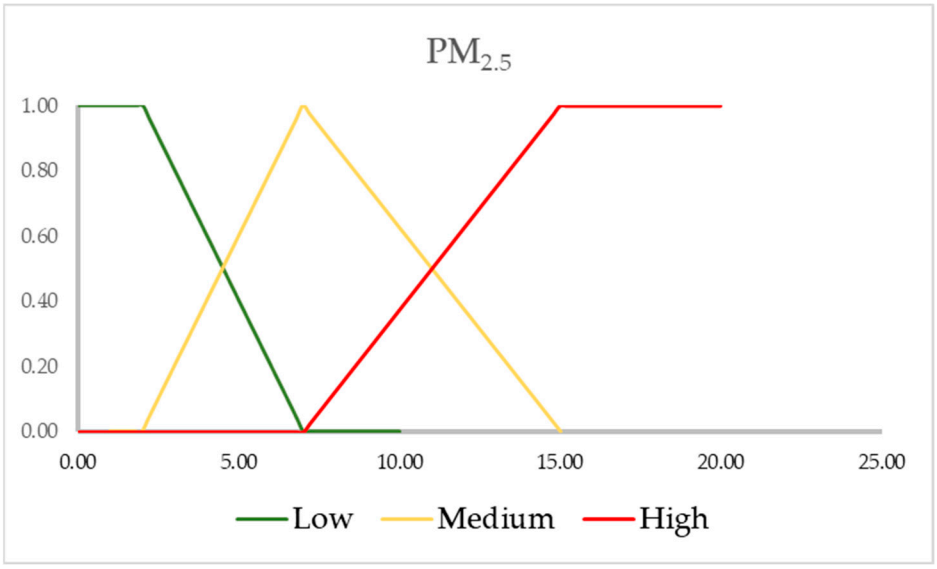

Figure 14. Fuzzy partition of $PM_{2.5}$.

Figure 14 shows the fuzzy partition of $PM_{2.5}$.

Executing the process described previously, the zones classified with $PM_{2.5}$ concentration High are detected as hotspots.

Finally, the $PM_{2.5}$ criticality map is created considering the criticality levels described in Table 2. Figure 15 shows this criticality map.

In this case, the hotspot areas extend to the entire city, and there are no areas with criticality level *Low*. Most of the areas are classified with criticality level *Medium*, while only some areas in the central area of the city, where the population density is *Medium* or *High*, are classified, respectively, with criticality level *High* and *Very High*.

Probably, the fact that the entire city constitutes a hotspot for the concentration of $PM_{2.5}$ is because this pollutant can remain suspended in the farmyard for a non-negligible period. Furthermore, since it consists of atmospheric particulate matter made up of particles with a smaller aerodynamic diameter than PM_{10}, it is even more dangerous for the health of inhabitants, as it manages to penetrate the lungs and, in some cases, reach the circulatory system. Therefore, the areas classified with *High* or *Very High* $PM_{2.5}$ criticality levels should be those of maximum alert for decision-makers.

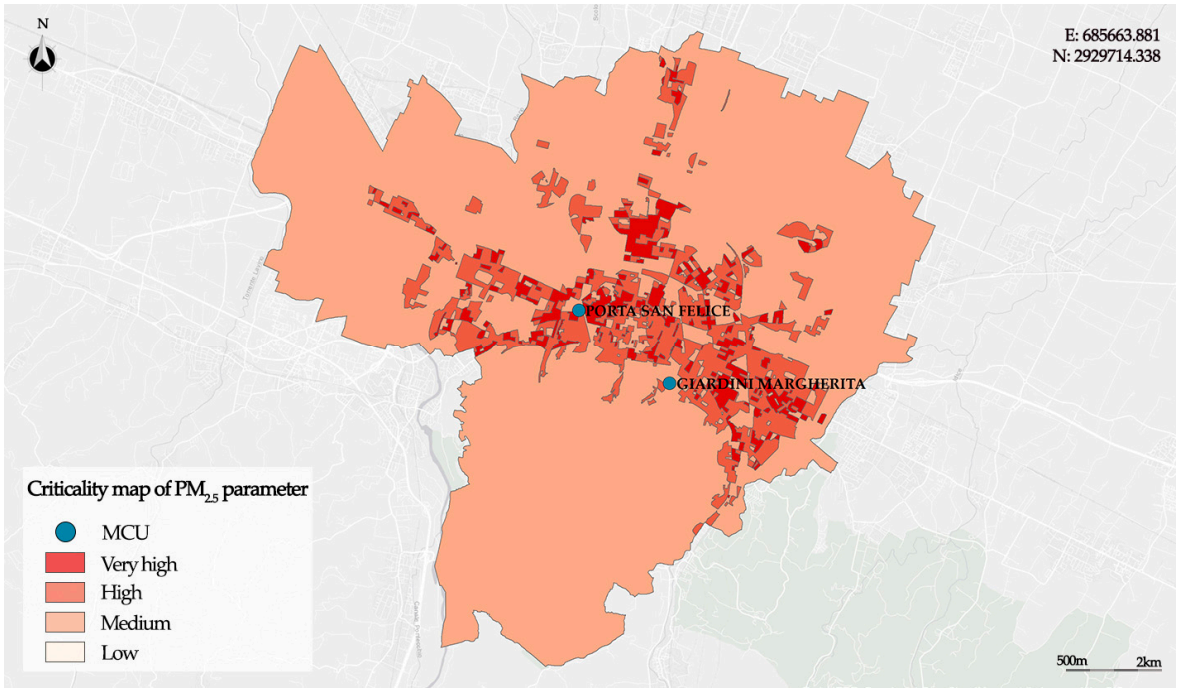

Figure 15. Criticality map of $PM_{2.5}$.

The results obtained for the three air pollutants highlight the usefulness of the framework as a decision support tool to determine which urban areas are most critical due to high concentrations of pollutants during periods of heatwaves. In particular, the criticality maps of the three pollutants show that central urban areas of the city of Bologna, with a high population density, are particularly critical. In the criticality map of $PM_{2.5}$, a very dangerous pollutant due to the respiratory and cardiovascular damage it can cause to the population, this central area of the city is very large; in it, the criticality due to the presence of the pollutant and the population density is High or Very High, suggesting the need for priority interventions to protect the health of citizens.

The obtained results align with peak values recorded by individual MCUs that exceed the WHO AQGs thresholds, as shown in Table 4. Furthermore, these results highlight that, compared to a traditional approach, which only reports alarm situations with values higher than the thresholds recorded by the MCU, the proposed framework approximates the spatial distribution of the parameter in the urban area of study. This allows for the detection of hotspots and the identification of the most critical urban areas.

4. Conclusions

The proposed framework allows for determining the most critical urban areas due to the concentration of pollutants in the air during periods of heatwaves. To ensure the portability of the framework also in urban settlements in which the monitoring of the area is carried out by fixed monitoring units, the urban study area is divided into Thiessen polygons built based on the positions of the monitoring units and is subsequently segmented into APASs, consisting of the spatial intersection between the census areas and the Thiessen polygons.

Each APAS is classified based on the exposed population density and the hazard of the pollutant concentration during the analyzed heatwave period, which is evaluated using a fuzzy-based approach. After having identified the urban areas most at risk due to the high concentration of the pollutant (hotspots), a map of the criticality of the pollutant is constructed in which the hotspots are classified by level of criticality assigned based on the density of the population at risk.

The framework was tested in the city of Bologna (Italy), analyzing the spatial distribution of PM_{10}, NO_2, and $PM_{2.5}$ concentrations during a heatwave period.

The criticality maps of the three air pollutants highlight that the central areas of the city, where the population density is high, are those where the health of citizens is most at risk.

This method has the advantage of being portable and flexible; it can be managed and customized very easily by local decision-makers for the analysis of the major critical issues generated by high concentrations of types of pollutants in the presence of heatwaves, providing decision analysis support in determining the main urban areas of intervention to protect the population at risk.

The limitation of the framework is represented by the fact that it is unsuitable in the presence of measurements with greater spatial resolution, for example, measurements carried out by mobile control units or using drones. In these cases, in fact, the segmentation of the study area into Thiessen polygons must be replaced by more sophisticated spatial modeling algorithms. For this reason, in future research, the framework will be tested on urban areas monitored with the use of mobile or drone-mounted control units, using more sophisticated spatial modeling methods to increase the spatial accuracy of the results. Furthermore, in the future, we intend to integrate our framework with hybrid deep learning and metaheuristic forecasting models to obtain more accurate predictions of the distribution of air pollutants in urban areas during heatwave periods, testing this framework on different urban settlements.

Author Contributions: Conceptualization, B.C., F.D.M. and V.M.; methodology, B.C., F.D.M. and V.M.; software, B.C., F.D.M. and V.M.; validation, B.C., F.D.M. and V.M.; formal analysis, B.C., F.D.M. and V.M.; investigation, B.C., F.D.M. and V.M.; resources, B.C., F.D.M. and V.M.; data curation, B.C., F.D.M. and V.M.; writing—original draft preparation, B.C., F.D.M. and V.M.; writing—review and editing, B.C., F.D.M. and V.M.; visualization, B.C., F.D.M. and V.M.; supervision, B.C., F.D.M. and V.M. All authors have read and agreed to the published version of the manuscript.

Funding: This research received no external funding.

Data Availability Statement: The data presented in this study are available on request from the corresponding author.

Conflicts of Interest: The authors declare no conflicts of interest.

References

1. Lelieveld, J.; Klingmüller, K.; Pozzer, A.; Poschl, U.; Fnais, M.; Daiber, A.; Münzel, T. Cardiovascular disease burden from ambient air pollution in Europe reassessed using novel hazard ratio functions. *Eur. Heart J.* **2019**, *40*, 1590–1596. [CrossRef]
2. Badach, J.; Voordeckers, D.; Nyka, L.; Van Acker, M. A framework for Air Quality Management Zones—Useful GIS-based tool for urban planning: Case studies in Antwerp and Gdańsk. *Build. Environ.* **2020**, *174*, 106743. [CrossRef]
3. He, B.-J.; Ding, L.; Prasad, D. Enhancing urban ventilation performance through the development of precinct ventilation zones: A case study based on the Greater Sydney, Australia Sustain. *Cities Soc.* **2019**, *47*, 101472. [CrossRef]
4. Oji, S.; Adamu, H. Air Pollution Exposure Mapping by GIS in Kano Metropolitan Area. *Pollution* **2021**, *7*, 101–112. [CrossRef]
5. D'Amato, G.; Vitale, C.; De Martino, A.; Viegi, G.; Lanza, M.; Molino, A.; Sanduzzi, A.; Vatrella, A.; Annesi-Maesano, I.; D'amato, M. Effects on asthma and respiratory allergy of Climate change and air pollution. *Multidiscip. Respir. Med.* **2015**, *10*, 39. [CrossRef]
6. Bartholy, J.; Pongrácz, R. A brief review of health-related issues occurring in urban areas related to global warming of 1.5 °C. *Curr. Opin. Environ. Sustain.* **2018**, *30*, 123–132. [CrossRef]
7. Lin, Y.-P.; Chu, H.-J.; Wu, C.-F.; Chang, T.-K.; Chen, C.-Y. Hotspot Analysis of Spatial Environmental Pollutants Using Kernel Density Estimation and Geostatistical Techniques. *Int. J. Environ. Res. Public Health* **2011**, *8*, 75–88. [CrossRef]
8. Pal, S.C.; Saha, A.; Chowdhuri, I.; Ruidas, D.; Chakrabortty, R.; Roy, P.; Shit, M. Earthquake hotspot and coldspot: Where, why and how? *Geosyst. Geoenviron.* **2023**, *2*, 100130. [CrossRef]
9. Cardone, B.; Di Martino, F. Fuzzy-Based Spatiotemporal Hot Spot Intensity and Propagation—An Application in Crime Analysis. *Electronics* **2022**, *11*, 370. [CrossRef]
10. Harirforoush, H.; Bellalite, L. A New Integrated GIS-based Analysis to Detect hot spots: A Case Study of the City of Sherbrooke. *Accid. Anal. Prev.* **2019**, *130*, 62–74. [CrossRef]
11. Cardone, B.; Di Martino, F. A New Geospatial Model Integrating a Fuzzy Rule-Based System in a GIS Platform to Partition a Complex Urban System in Homogeneous Urban Contexts. *Geosciences* **2018**, *8*, 440. [CrossRef]

12. Li, L.; Gong, J.; Zhou, J. Spatial Interpolation of Fine Particulate Matter Concentrations Using the Shortest Wind-Field Path Distance. *PLoS ONE* **2014**, *9*, e96111. [CrossRef]
13. Wong, D.; Yuan, L.; Perlin, S. Comparison of spatial interpolation methods for the estimation of air quality data. *J. Expo. Sci. Environ. Epidemiol.* **2004**, *14*, 404–415. [CrossRef]
14. Xingzhe, X.; Semanjski, I.; Gautama, S.; Tsiligianni, E.; Deligiannis, N.; Rajan, R.T.; Pasveer, F.; Philips, W. A Review of Urban Air Pollution Monitoring and Exposure Assessment Methods. *Int. J. Geoinform.* **2017**, *6*, 389. [CrossRef]
15. Liu, X.; Ye, F.; Liu, Y.; Xie, X.; Fan, J. Real-Time Forecasting Method of Urban Air Quality Based on Observation Sites and Thiessen Polygons. *Int. J. Smart Sens. Intell. Syst.* **2015**, *8*, 2065–2082. [CrossRef]
16. Verghese, S.; Nema, A.K. Assessment of Air Quality Monitoring Network for Adequacy in Representation of Urban $PM_{2.5}$ and Coverage Efficiency: A Case Study of Delhi, India. *Environ. Eng. Sci.* **2023**, *40*, 373–380. [CrossRef]
17. Navares, L.; Aznarte, J.L. Predicting air quality with deep learning LSTM: Towards comprehensive models. *Ecol. Inform.* **2020**, *55*, 101019. [CrossRef]
18. Mao, W.; Wang, W.; Jiao, L.; Zhao, S.; Liu, A. Modeling air quality prediction using a deep learning approach: Method optimization and evaluation Sustainable. *Cities Soc.* **2021**, *65*, 102567. [CrossRef]
19. Bacanin, B.N.; Sarac, M.; Budimirovic, N.; Zivkovic, M.; AlZubi, A.A.; Bashir, A.K. Smart wireless health care system using graph LSTM pollution prediction and dragonfly node localization. *Sustain. Comput. Inform. Syst.* **2022**, *35*, 100711. [CrossRef]
20. Lavana, H.; Prathik, N.R. Deep Learning-Based Air Pollution Forecasting System Using Multivariate LSTM. In *Artificial Intelligence Tools and Technologies for Smart Farming and Agriculture Practices*; Gupta, R.K., Jain, A., Wang, J., Bharti, S.K., Patel, S., Eds.; IGI Global Publishing: Beijing, China, 2023; pp. 101–114. [CrossRef]
21. Drewil, G.I.; Al-Bahadili, R.J. Air pollution prediction using LSTM deep learning and metaheuristics algorithms. *Meas. Sens.* **2022**, *24*, 100546. [CrossRef]
22. Carbajal-Hernández, J.J.; Sánchez-Fernández, L.P.; Carrasco-Ochoa, J.A.; Martínez-Trinidad, J.F. Assessment and prediction of air quality using fuzzy logic and autoregressive models. *Atmos. Environ.* **2012**, *60*, 37–50. [CrossRef]
23. Alyousifi, Y.; Othman, M.; Sokkalingam, R.; Faye, I.; Silva, P.C.L. Predicting Daily Air Pollution Index Based on Fuzzy Time Series Markov Chain Model. *Symmetry* **2020**, *12*, 293. [CrossRef]
24. Cardone, B.; Di Martino, F. GIS-based hierarchical fuzzy multicriteria decision-making method for urban planning. *J. Ambient. Intell. Humaniz. Comput.* **2021**, *12*, 601–615. [CrossRef]
25. Cardone, B.; D'Ambrosio, V.; Di Martino, F.; Miraglia, V. Hierarchical Fuzzy MCDA Multi-Risk Model for Detecting Critical Urban Areas in Climate Scenarios. *Appl. Sci.* **2024**, *14*, 3066. [CrossRef]
26. World Health Organization. WHO Global Air Quality Guidelines: Particulate Matter ($PM_{2.5}$ and PM_{10}) , Ozone, Nitrogen Dioxide, Sulfur Dioxide and Carbon Monoxide. World Health Organization. 2021. Available online: https://iris.who.int/handle/10665/345329 (accessed on 1 May 2024).
27. Ruspini, E.H. A new approach to clustering. *Inf. Control.* **1969**, *15*, 22–32. [CrossRef]